TÜBİTAK

Turkish Journal of Physics

http://journals.tubitak.gov.tr/physics/

Research Article

Turk J Phys
(2017) 41: 560 – 575

doi:10.3906/fiz-1707-19

Applying a self-feedback method to control chaos in the Buck converter

Meimei JIA*
Department of Automation, School of Electric Power, Jinchuan Campus, Inner Mongolia University of Technology, Hohhot, P.R. China

Received: 24.07.2017 • **Accepted/Published Online:** 23.08.2017 • **Final Version:** 18.12.2017

Abstract: Chaos exists in the Buck converter due to the switching action of the controlled switch and this nonlinear phenomenon results in unreliable working performances. Hence, this paper uses a self-feedback control method with two adjustable parameters to suppress the chaotic behavior in the Buck converter. First, the self-feedback control method is presented by introducing a generic second-order chaotic system. Then, from the perspective of transfer functions obtained in terms of the piecewise linear model of the controlled Buck converter, effects of controller's parameters on system performances are discussed. On the basis of the Jacobian matrix of the discrete iterative mapping model of the controlled Buck converter, the stability of the period-1 orbit is analyzed. Finally, numerical simulations confirm that without determining targeting orbits in advance, this self-feedback control method can stabilize the chaotic behavior of the Buck converter to the stable period-1 orbit.

Key words: Chaos control, Buck converter, transfer function, self-feedback

1. Introduction

The Buck converter, which converts a direct current (DC) voltage to a lower DC voltage, has strong nonlinearity. This system exhibits some complex nonlinear phenomena such as chaos, bifurcation, and quasi-periodicity [1–3]. For example, with the increasing of the input voltage, the Buck converter undergoes period-1, -2, and -4 orbits and eventually goes into the chaotic region. The chaotic phenomenon can pose a threat to the stability of the Buck converter. Thus, it is necessary to control chaos in the Buck converter. Control of chaos involves designing a control law that is capable of stabilizing the chaotic behavior to a fixed point or various periodic trajectories.

After the OGY method as the pioneering work was developed [4], there have been many other ideas about controlling chaos. Generally, these chaos control methods may be classified into two main groups: one is feedback control [5–8] and the other is non-feedback control [9,10]. For the non-feedback control, the chaotic behavior is eliminated by adopting weak periodic perturbations and parameter perturbations. However, non-feedback control alters intrinsic characteristics of the original dynamical system. Feedback control has been extensively applied because of its sound theoretical basis and better performance. Feedback control can hold intrinsic characteristics.

There are several feedback control methods that are appropriate to control the chaotic phenomenon existing in the Buck converter. The time-delayed feedback control method, which does not require the knowledge of the target orbits [11,12], has been used to control chaos in the Buck converter. Its controller is constructed on the basis of the difference between the current state and the time-delayed state. From the frequency-domain

*Correspondence: meimeijia14@163.com

perspective, based on the notch filter, Lu's research group has studied several effective feedback control methods as well as similar methods for controlling chaos in the Buck converter [13–16]. The input of the controller was chosen from the state variable or the output for detecting the nonlinear behaviors of the controlled system. These feedback control methods [11–16] require full or partial state variables of the system.

Based on an idea borrowed from "iteration", which can be usually found in discrete dynamical systems, this paper provides a self-feedback chaos control method to control chaos in the Buck converter that belongs to hybrid dynamical systems. The self-feedback control process can be understood as a substitution process, like the first iteration.

Differing from previous methods [11–16], the self-feedback chaos control method in this paper does not depend on the state variables of the system. Compared to the classical targeting method [17], without calculating targeting orbits beforehand, the self-feedback chaos control method can stabilize the chaotic behavior in the Buck converter to the stable period-1 orbit. The washout filter has to supplement a dimension based on that of the original system to realize chaos control for the Buck converter [18], but the self-feedback chaos control method does not need to add a dimension.

The rest of the paper is organized as follows. Section 2 reviews the fact that chaotic behavior exists in the Buck converter. In Section 3, a self-feedback chaos control method is addressed. In Section 4, first, introducing the self-feedback chaos control method to the original Buck converter, the model of the controlled Buck converter is established. In terms of this model, transfer functions corresponding to the controlled switch G being on or off are given. Then, from the perspective of the transfer functions, effects of the controller's parameters on system performances are discussed. In Section 5, the stability of the period-1 orbit is analyzed using the Jacobian matrix. Section 6 implements numerical simulations. In the end, the paper gives the concluding remarks.

2. System description and overview of the route to chaos

Figure 1 shows the topological graph of the Buck converter. For convenience in obtaining the circuit state equations, we assume that all the components in the circuit are idealized. Comparator A_2 has an infinite gain. The switches have zero ON and infinite OFF resistances, and they can switch on or off instantly without time delay.

In this paper, the Buck converter operates in continuous conduction mode.

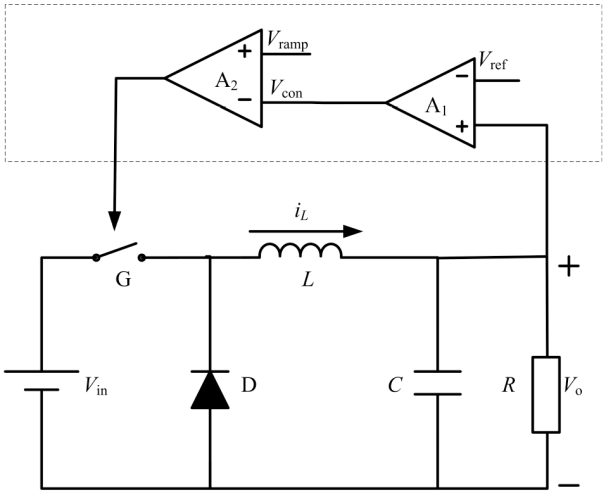

Figure 1. Topological graph of the Buck converter.

Assuming that error amplifier A_1 works in the linear region, its output, known as the control voltage, is given by:

$$V_{con}(t) = \alpha [V_o(t) - V_{ref}], \tag{1}$$

where α is the gain of A_1 and V_{ref} denotes the reference voltage. The control voltage V_{con} and the sawtooth voltage V_{ramp} are connected to two input ports of comparator A_2. The sawtooth voltage is described by [19]:

$$V_{ramp}(t) = V_L + (V_H - V_L)\left(\frac{t}{T} \bmod 1\right), \tag{2}$$

where V_H and V_L are the upper and lower voltages of V_{ramp}, respectively, and T is the switching period, i.e. the period of V_{ramp}. If $V_{ramp} > V_{con}$, then comparator A_2 generates a high level such that switch G is on. If $V_{ramp} < V_{con}$, A_2 yields a low level such that it is off.

Considering the inductor current i_L and the output voltage V_o as state variables, the circuit state equations, known as the piecewise linear model, corresponding to the ON and OFF states of the controlled switch G are:

$$\begin{array}{l} \dot{i}_L = \frac{-V_o}{L} + \frac{V_{in}}{L}u \\ \dot{V}_o = \frac{i_L}{C} - \frac{V_o}{R \times C} \end{array}, \tag{3}$$

where V_{in} is the input voltage, R is the resistance, L is the inductance, and C is the capacitance. In Eq. (3), the switching logic u is:

$$\begin{cases} u = 1, & V_{ramp} > V_{con} \\ u = 0, & V_{ramp} < V_{con} \end{cases}. \tag{4}$$

Circuit parameters [19,20] are: $V_{in} = 18 - 45\,V$, $R = 22\,\Omega$, $L = 20\,mH$, $C = 47\,\mu F$, $T = 400\,\mu s$, $V_{ref} = 11.3\,V$, $\alpha = 8.4$, $V_L = 3.8\,V$, and $V_H = 8.2\,V$.

On the basis of Eq. (3), the global bifurcation process is obtained (see Figure 2). It is admittedly found that with the input voltage V_{in} increasing (here, V_{in} is considered as a bifurcation parameter), the Buck converter undergoes the period-doubling bifurcation process and eventually goes into the chaotic region.

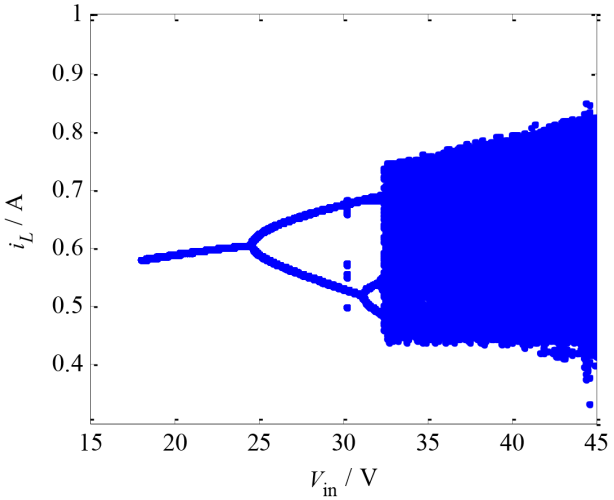

Figure 2. Global bifurcation process in the Buck converter ($V_{in} = 18 - 45\,V$), inductor current versus the input voltage.

From Figure 2, obviously, when $V_{in} = 32.35 - 45\,V$ the system is in the chaotic state. In the following text, without loss of generality, taking $V_{in} = 35 - 40V$, the chaotic state is discussed using the inductor current

waveform, the output voltage waveform, the switching logic, the power-spectral density (PSD), the Poincare section, and the largest Lyapunov exponent (LLE).

In Figures 3a and 3b, the inductor current waveform and the output voltage waveform oscillate irregularly. In Figure 3c, the switching logic is aperiodic. This means that the controlled switch G switches between the OFF state and the ON state irregularly. The PSD based on fast Fourier transform (FFT) behaves as a continuous spectrum with background noise (see Figure 3d). The Poincare section has strange attractors (see Figure 3e). The largest Lyapunov exponent $\lambda_{\max}$ is greater than zero while the Buck converter is in the chaotic state, as shown in Figure 3f.

3. Self-feedback chaos control method

First, for simplification, consider a second-order system with existing chaotic phenomenon:

$$\frac{dx_1}{dt} = f_1(x_1, x_2, t); \tag{5a}$$

$$\frac{dx_2}{dt} = f_2(x_1, x_2, t). \tag{5b}$$

For Eq. (5), a self-feedback chaos control method (its block diagram is shown in Figure 4) with two adjustable control parameters γ and m is designed as:

$$\bar{f}_1(x_1, x_2, t) = m \times \gamma + (1 - m) \times f_1(x_1, x_2, t); \tag{6a}$$

$$\bar{f}_2(x_1, x_2, t) = m \times \gamma + (1 - m) \times f_2(x_1, x_2, t), \tag{6b}$$

where $\gamma > 0$, and the control intensity is $0 \leq m < 1$.

Introducing the self-feedback chaos control method in Eq. (6) to the original chaotic system of Eq. (5), or in other words substituting $\bar{f}_1(x_1, x_2, t)$, $\bar{f}_2(x_1, x_2, t)$ for $f_1(x_1, x_2, t)$, $f_2(x_1, x_2, t)$ respectively (here the substituting process corresponds to the first iteration in discrete dynamical systems), the controlled system is given by:

$$\frac{dx_1}{dt} = m \times \gamma + (1 - m) \times f_1(x_1, x_2, t); \tag{7a}$$

$$\frac{dx_2}{dt} = m \times \gamma + (1 - m) \times f_2(x_1, x_2, t). \tag{7b}$$

In Eq. (7), if $m = 0$, the controlled system of Eq. (7) reduces to the original chaotic system of Eq. (5). If $\gamma > 0$, $0 < m < 1$, the self-feedback chaos control method is fed back to the original chaotic system such that this system evolves under controlled circumstances.

4. Transfer functions and effects of the controller's parameters on system performances

In this section, first, based on the piecewise linear model of the controlled Buck converter, transfer functions are obtained. Secondly, we analyze the effects of the controller's parameters on system performances. Finally, to improve voltage conversion efficiency in the process of carrying out chaos control, the range of parameter γ is discussed.

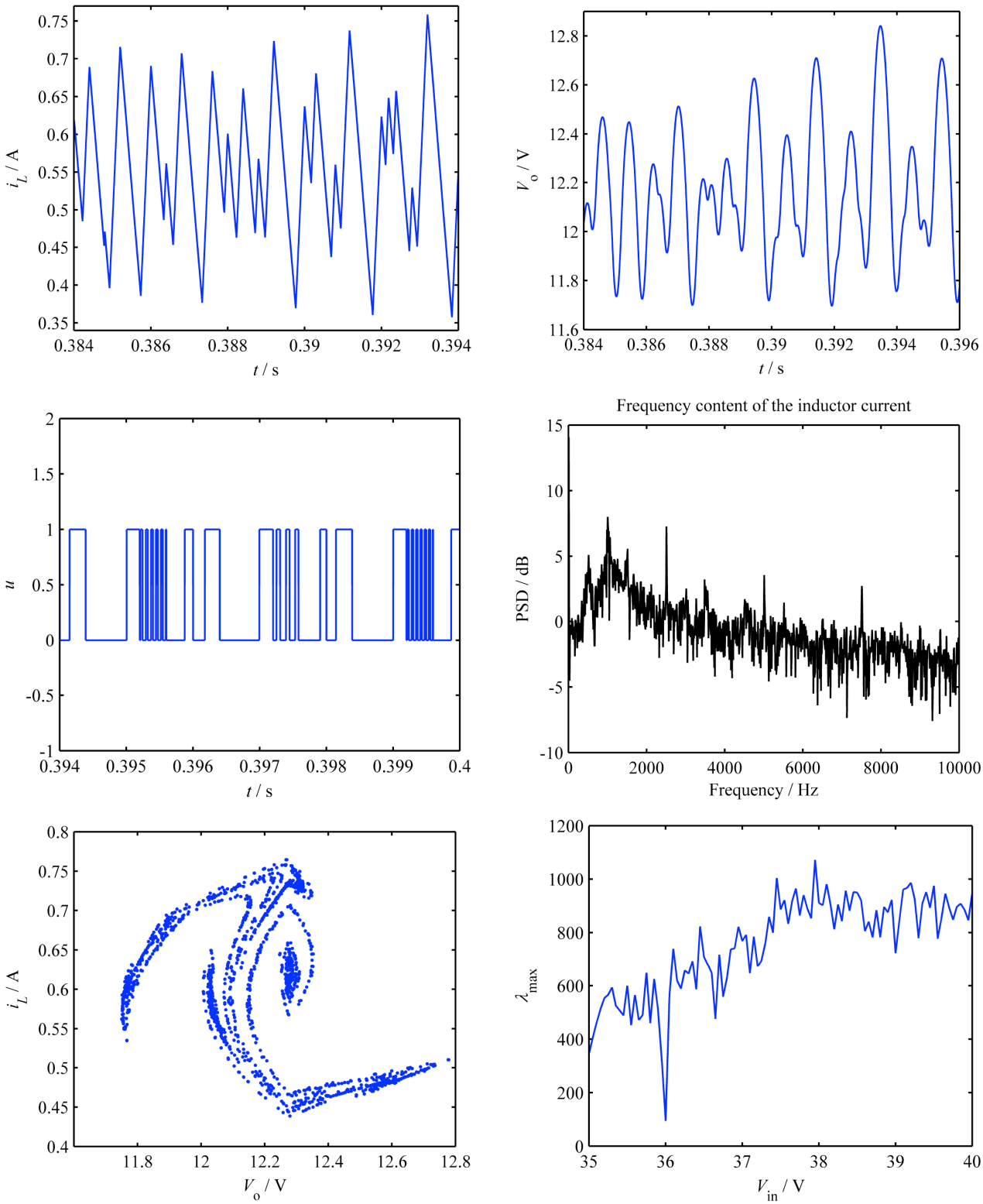

Figure 3. Chaotic state: (a) inductor current waveform of the chaotic state ($V_{in} = 35\,V$); (b) output voltage waveform of the chaotic state ($V_{in} = 35\,V$); (c) switching logic diagram of the chaotic state ($V_{in} = 35\,V$) (d) PSD of the chaotic state ($V_{in} = 35\,V$), where power-spectral density is abbreviated as PSD; (e) Poincare section of the chaotic state ($V_{in} = 35\,V$); (f) largest Lyapunov exponent $\lambda_{\max}$ ($V_{in} = 35 - 40\,V$).

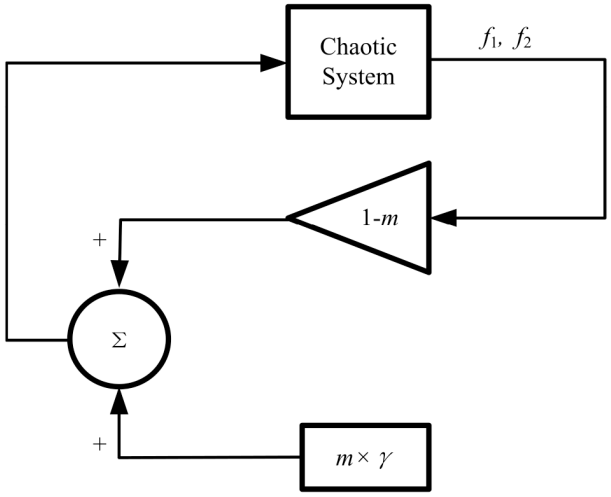

Figure 4. Block diagram of the self-feedback chaos control method.

Clearly, adding the self-feedback chaos control method of Eq. (6) into the original Buck converter of Eq. (3), the piecewise linear model of the controlled Buck converter is given by:

$$\dot{i}_L = m \times \gamma + (1-m) \times \left(\frac{-V_o}{L} + \frac{V_{in}}{L} u \right); \tag{8a}$$

$$\dot{V}_o = m \times \gamma + (1-m) \times \left(\frac{i_L}{C} - \frac{V_o}{R \times C} \right). \tag{8b}$$

From Eqs. (8a) and (8b), if $u = 1$ (the controlled switch G is on), then the controlled Buck converter is:

$$\dot{i}_L = m \times \gamma - (1-m) \times \frac{V_o}{L} + (1-m) \times \frac{V_{in}}{L}, \tag{9a}$$

$$\dot{V}_o = m \times \gamma + (1-m) \times \frac{i_L}{C} - (1-m) \times \frac{V_o}{R \times C}. \tag{9b}$$

Let $\gamma = \delta \times V_{in}$ where $\delta > 0$. According to Eq. (9), the transfer function from output voltage V_o to input voltage V_{in} is:

$$H_{on}(s) = \frac{V_o}{V_{in}} = \frac{\frac{L \times \delta \times m \times (1-m) + (1-m)^2}{L \times C}}{s^2 + \frac{(1-m)s}{R \times C} + \frac{(1-m)^2}{L \times C}}. \tag{10}$$

We know that for the second-order system, the standard form of the transfer function is:

$$G(s) = \frac{k_0 \times \omega_n^2}{s^2 + 2\xi \times \omega_n \times s + \omega_n^2} \quad , \tag{11}$$

where k_0 is the amplification factor. ω_n is the natural frequency. ξ is the damping ratio. Let $H_{on}(s) = G(s)$. We get $k_0 = 1 + \frac{L \times \delta \times m}{1-m}$, $\omega_n = \frac{1-m}{\sqrt{L \times C}}$, and $\xi = \frac{\frac{1-m}{R \times C}}{2\omega_n} = \frac{1}{2R}\sqrt{\frac{L}{C}}$.

Similarly, from Eqs. (8a) and (8b), if $u = 0$ (the controlled switch G is off), then the controlled Buck converter is:

$$\dot{i}_L = m \times \gamma + (1-m) \times \frac{-V_o}{L}, \tag{12a}$$

$$\dot{V}_o = m \times \gamma + (1-m) \times \frac{i_L}{C} - (1-m) \times \frac{V_o}{R \times C}. \tag{12b}$$

Based on Eq. (12), the transfer function is:

$$H_{off}(s) = \frac{V_o}{V_{in}} = \frac{\frac{\delta \times m \times (1-m)}{C}}{s^2 + \frac{(1-m)s}{R \times C} + \frac{(1-m)^2}{L \times C}}. \tag{13}$$

Let $H_{off}(s) = G(s)$. We get $k_0 = \frac{L \times \delta \times m}{1-m}$, $\omega_n = \frac{1-m}{\sqrt{L \times C}}$, and $\xi = \frac{1}{2R}\sqrt{\frac{L}{C}}$.

From the transfer functions of Eqs. (10) and (13), we can obtain three results.

First, we know that the controlled Buck converter has two closed-loop poles:

$$s_{1,2} = -\xi \times \omega_n \pm j\omega_d, \tag{14}$$

where $\omega_d = \omega_n\sqrt{1-\xi^2}$ is the vibrational frequency. Because of $\omega_d = (1-m)\sqrt{\frac{1-\xi^2}{L \times C}}$, the larger m is, the smaller ω_d is. That is, while the control intensity m increases, the system response becomes smoother.

Second, the distance d between the closed-loop poles and the imaginary axis is:

$$\begin{array}{l} d = \xi \times \omega_n = \\ \xi \times \frac{1-m}{\sqrt{L \times C}} \end{array}. \tag{15}$$

From Eq. (15), the larger m is, the smaller d is. According to classical control theory, if the closed-loop poles are closer to the imaginary axis, then these poles have a greater influence on the system. This implies that with m increasing the control action that imposes on the system becomes stronger.

Finally, γ has no effect on the smoothness of the system response since this parameter is merely related to the amplification factor k_0. It is well known that k_0 is independent of the smoothness.

Voltage conversion efficiency [21] is defined as $\eta = \bar{V}_o/V_{in}$, where the over bar stands for the averaged output voltage. From Figure 5, it can be seen that when the input voltage V_{in} increases, voltage conversion efficiency η decreases in a general trend. It hints that we can diminish V_{in} to improve this efficiency.

Substituting $\gamma = \delta \times V_{in}$ into Eq. (9a), Eq. (9b) becomes:

$$\dot{i}_L = V_{in}\left(m \times \delta + \frac{1-m}{L}\right) + (1-m) \times \frac{-V_o}{L}. \tag{16}$$

When the control action is not activated ($m = 0$), the term $V_{in}\left(m \times \delta + \frac{1-m}{L}\right)$ in Eq. (16) reduces to $\frac{V_{in}}{L}$. To diminish V_{in}, the condition $0 < V_{in}\left(m \times \delta + \frac{1-m}{L}\right) < \frac{V_{in}}{L}$ should be satisfied. That is, the new input voltage $\widehat{V}_{in} = V_{in}(m \times \delta \times L + 1 - m)$ after the Buck converter being controlled is lower than the original input voltage V_{in}. Then $0 < \delta < \frac{1}{L}$ is obtained ($0 < \gamma < \frac{V_{in}}{L}$). Thus, the range of $\gamma > 0$ is narrowed to $0 < \gamma < \frac{V_{in}}{L}$, which is convenient to tune γ in the process of implementing numerical simulations.

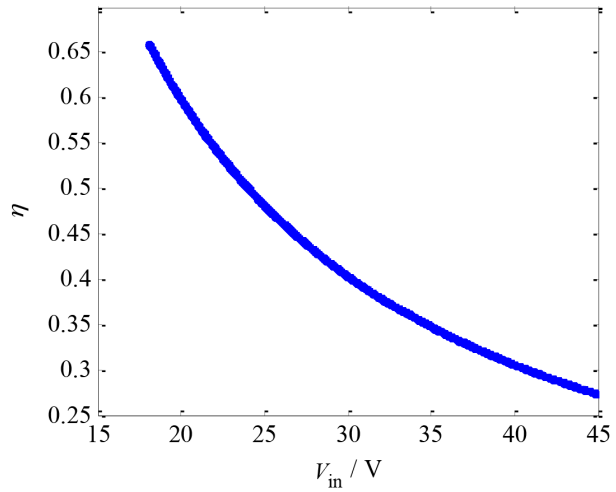

Figure 5. Voltage conversion efficiency η versus the input voltage V_{in}.

From $0 < \gamma < \frac{V_{in}}{L}$, we know that the smaller γ is, the lower V_{in} is and the higher η is. Note that the range of the input voltage V_{in} should guarantee that the uncontrolled system is under the chaotic regime.

5. Stability analysis of the period-1 orbit

In this section, we establish the discrete iterative mapping model of the controlled Buck converter and then discuss the stability of the period-1 orbit based on the Jacobian matrix. We will give more detailed analyses using numerical simulations later.

Rewrite Eq. (8) as:

$$\begin{bmatrix} \dot{V}_o \\ \dot{i}_L \end{bmatrix} = (1-m)\begin{bmatrix} \frac{-1}{R\times C} & \frac{1}{C} \\ \frac{-1}{L} & 0 \end{bmatrix}\begin{bmatrix} V_o \\ i_L \end{bmatrix} + (1-m)\times\begin{bmatrix} 0 \\ \frac{1}{L} \end{bmatrix} V_{in}\times u + \begin{bmatrix} 1 \\ 1 \end{bmatrix} m\times\gamma. \tag{17}$$

Letting $\gamma = \delta \times V_{in}$, $\frac{m\times\delta}{1-m} = \overline{\delta}$ and Eq. (17) becomes:

$$\begin{bmatrix} \dot{V}_o \\ \dot{i}_L \end{bmatrix} = (1-m)\begin{bmatrix} \frac{-1}{R\times C} & \frac{1}{C} \\ \frac{-1}{L} & 0 \end{bmatrix}\begin{bmatrix} V_o \\ i_L \end{bmatrix} + (1-m)\times\begin{bmatrix} \overline{\delta} \\ \frac{u}{L}+\overline{\delta} \end{bmatrix} V_{in}, \tag{18}$$

where:

$$\mathbf{A}_{on} = \mathbf{A}_{off} = (1-m)\begin{bmatrix} \frac{-1}{R\times C} & \frac{1}{C} \\ \frac{-1}{L} & 0 \end{bmatrix},$$

$$\begin{aligned} \mathbf{B}_{on} &= (1-m)\begin{bmatrix} \overline{\delta} \\ \frac{1}{L}+\overline{\delta} \end{bmatrix} \\ \mathbf{B}_{off} &= (1-m)\begin{bmatrix} \overline{\delta} \\ \overline{\delta} \end{bmatrix} \end{aligned}.$$

We discretize the state variables by means of the stroboscopic mapping method, which can be obtained by observing the system dynamics every T seconds, at the beginning of each V_{ramp} cycle. Note that $x_n = x(nT) = [V_o(nT), i_L(nT)]^T$, $n = 1, 2, 3\cdots$. In each cycle (for example, $T \sim 2T$), the Buck converter goes through two kinds of phases.

1) The controlled switch G is under the OFF phase if $T \sim T_s$. When this phase is over, the state variable x_m is:

$$x_m = f_{off}\left(x_n, \bar{d}_n\right) = \mathbf{N}_{off}\left(\bar{d}_n\right) \times x_n + \mathbf{M}_{off}\left(\bar{d}_n\right) \times V_{in}, \tag{19}$$

where $\bar{d}_n = 1 - d_n$, d_n represents the duty ratio, which is defined as the ratio of the ON duration to the switching period T.

2) The controlled switch G is under the ON phase if $T_s \sim 2T$. When this phase is over, the state variable x_{n+1} is:

$$x_{n+1} = f_{on}\left(x_m, \bar{d}_n\right) = \mathbf{N}_{on}\left(1 - \bar{d}_n\right) \times x_m + \mathbf{M}_{on}\left(1 - \bar{d}_n\right) \times V_{in}. \tag{20}$$

Incorporating Eqs. (19) and (20), the discrete iterative mapping model of the controlled Buck converter is given by:

$$x_{n+1} = f\left(x_n, \bar{d}_n\right) = N_{on}\left(1 - \bar{d}_n\right) \times N_{off}\left(\bar{d}_n\right) \times x_n + \left[N_{on}\left(1 - \bar{d}_n\right) \times M_{off}\left(\bar{d}_n\right) + M_{on}\left(1 - \bar{d}_n\right)\right] \times V_{in}, \tag{21}$$

where:

$$N_{on}\left(1 - \bar{d}_n\right) = e^{\mathbf{A}_{on} \times d_n \times T};$$

$\mathbf{M}_{on}\left(1 - \bar{d}_n\right) = \mathbf{A}_{on}^{-1}\left[\mathbf{N}_{on}\left(1 - \bar{d}_n\right) - \mathbf{I}\right]\mathbf{B}_{on}$, $\mathbf{I}$ represents the identity matrix;

$$\mathbf{N}_{off}\left(\bar{d}_n\right) = e^{\mathbf{A}_{off} \times \bar{d}_n \times T};$$

$$\mathbf{M}_{off}\left(\bar{d}_n\right) = \mathbf{A}_{off}^{-1}\left[\mathbf{N}_{off}\left(\bar{d}_n\right) - \mathbf{I}\right]\mathbf{B}_{off}.$$

In addition, from Eqs. (1) and (2), the function of the duty ratio, known as the switching logic, is defined as:

$$u\left(\bar{d}_n\right) = V_{con}\left(\bar{d}_n\right) - V_{ramp}\left(\bar{d}_n\right). \tag{22}$$

The Jacobian matrix of Eq. (21), $\mathbf{\Gamma}$, is given by:

$$\mathbf{\Gamma} = \frac{\partial x_{n+1}}{\partial x_n} = \frac{\partial f}{\partial x_n} - \frac{\partial f}{\partial \bar{d}_n}\left(\frac{\partial u}{\partial \bar{d}_n}\right)^{-1}\frac{\partial u}{\partial x_n} \quad , \tag{23}$$

where:

$$\begin{aligned}
\frac{\partial f}{\partial x_n} =& \mathbf{N}_{on}\left(1-\bar{d}_n\right)\times\mathbf{N}_{off}\left(\bar{d}_n\right)\\
\frac{\partial f}{\partial \bar{d}_n} =& \left[\frac{\partial \mathbf{N}_{on}\left(1-\bar{d}_n\right)}{\partial \bar{d}_n}\mathbf{N}_{off}\left(\bar{d}_n\right)+\mathbf{N}_{on}\left(1-\bar{d}_n\right)\times\frac{\partial \mathbf{N}_{off}\left(\bar{d}_n\right)}{\partial \bar{d}_n}\right]x_n\\
&+\left[\frac{\partial \mathbf{N}_{on}\left(1-\bar{d}_n\right)}{\partial \bar{d}_n}\mathbf{M}_{off}\left(\bar{d}_n\right)+\mathbf{N}_{on}\left(1-\bar{d}_n\right)\times\frac{\partial \mathbf{M}_{off}\left(\bar{d}_n\right)}{\partial \bar{d}_n}+\frac{\partial \mathbf{M}_{on}\left(1-\bar{d}_n\right)}{\partial \bar{d}_n}\right]V_{in}\\
=&\left[-\mathbf{A}_{on}\times T\times\mathbf{N}_{on}\left(1-\bar{d}_n\right)\times\mathbf{N}_{off}\left(\bar{d}_n\right)+\mathbf{N}_{on}\left(1-\bar{d}_n\right)\times\mathbf{A}_{off}\times T\times\mathbf{N}_{off}\left(\bar{d}_n\right)\right]x_n\\
&+\left[-\mathbf{A}_{on}\times T\times\mathbf{N}_{on}\left(1-\bar{d}_n\right)\times\mathbf{M}_{off}\left(\bar{d}_n\right)+\mathbf{N}_{on}\left(1-\bar{d}_n\right)\times\mathbf{N}_{off}\left(\bar{d}_n\right)\times\mathbf{B}_{off}\right.\\
&\left.\times T-\mathbf{N}_{on}\left(1-\bar{d}_n\right)\times\mathbf{B}_{on}\times T\right]V_{in}\\
\frac{\partial u}{\partial \bar{d}_n} =& \left[\alpha\ 0\right]\left[\mathbf{A}_{off}\times T\times\mathbf{N}_{off}\left(\bar{d}_n\right)\times x_n+T\times\mathbf{N}_{off}\left(\bar{d}_n\right)\times\mathbf{B}_{off}\times V_{in}\right]-\left(V_H-V_L\right)T\\
=&\left[\alpha\ 0\right]\mathbf{N}_{off}\left(\bar{d}_n\right)\left(\mathbf{A}_{off}\times x_n+\mathrm{B}_{off}\times V_{in}\right)T-\left(V_H-V_L\right)T\\
\frac{\partial u}{\partial x_n} =& \left[\alpha\ 0\right]\mathbf{N}_{off}\left(\bar{d}_n\right)
\end{aligned}$$

In terms of $\det\left[\lambda\times\mathbf{I}-\mathbf{\Gamma}\right]$, the characteristic multipliers λ_1, λ_2 can be calculated. If $|\lambda_i|<1,\ i=1,2$ are less than 1, then the period-1 orbit is stable, while one characteristic multiplier greater than 1 suffices to render the periodic orbit unstable. In particular, if one characteristic multiplier equals –1 and the other is less than 1, the period-doubling bifurcation occurs. In this way, the stability of the period-1 orbit is analyzed based on the Jacobian matrix.

6. Numerical simulations

In this section, numerical simulations are performed to verify whether the chaotic behavior in the Buck converter can be controlled to the stable period-1 orbit via applying the self-feedback chaos control method and to verify the correctness of the theories given in Sections 4 and 5.

Circuit parameters are: $V_{in}=35-40\,V$, $R=22\,\Omega$, $L=20\,mH$, $C=47\,\mu F$, $T=400\,\mu s$, $V_{ref}=11.3\,V$, $\alpha=8.4$, $V_L=3.8\,V$, and $V_H=8.2\,V$. The controller's parameters are $0<m<1$, $0<\gamma<\frac{V_{in}}{L}$.

Figure 6 shows the evolutionary process of the output voltage V_o from the chaotic state to the various periodic orbits with control intensity m increasing, taking $\gamma=4$, $V_{in}=35\,V$. It can be observed that the controlled Buck converter undergoes the chaotic state, and then undergoes the period-4, -2, and -1 orbits (an inverse period-doubling bifurcation process). Note that there are some coexisting attractors around $m=0.14$ and $m=0.31$.

Figure 7a shows that when $m=0.4-0.25$, characteristic multipliers all lie within the unit circle in the complex plane. We conclude that the period-1 orbit is stable. It is worth noting that when m is about 0.31, coexisting attractors occur and the corresponding characteristic multipliers lie in the right half of the complex plane.

From Figure 7b, when the control intensity m decreases from 0.25 to 0.2046, two conjugate characteristic multipliers are closer to the real axis and arrive at the real axis. Then the characteristic multipliers break away, one turning left and the other turning right. The left characteristic multiplier eventually exits the unit circle

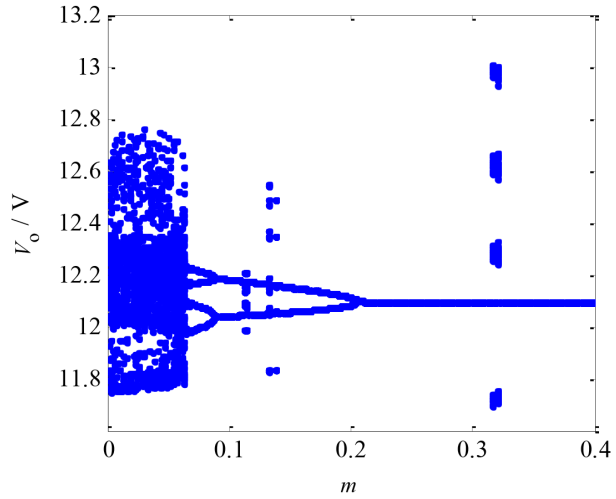

Figure 6. Evolutionary process of the output voltage from the chaotic state to the various periodic orbits with the control intensity m increasing, taking $\gamma = 4$, $V_{in} = 35\,V$.

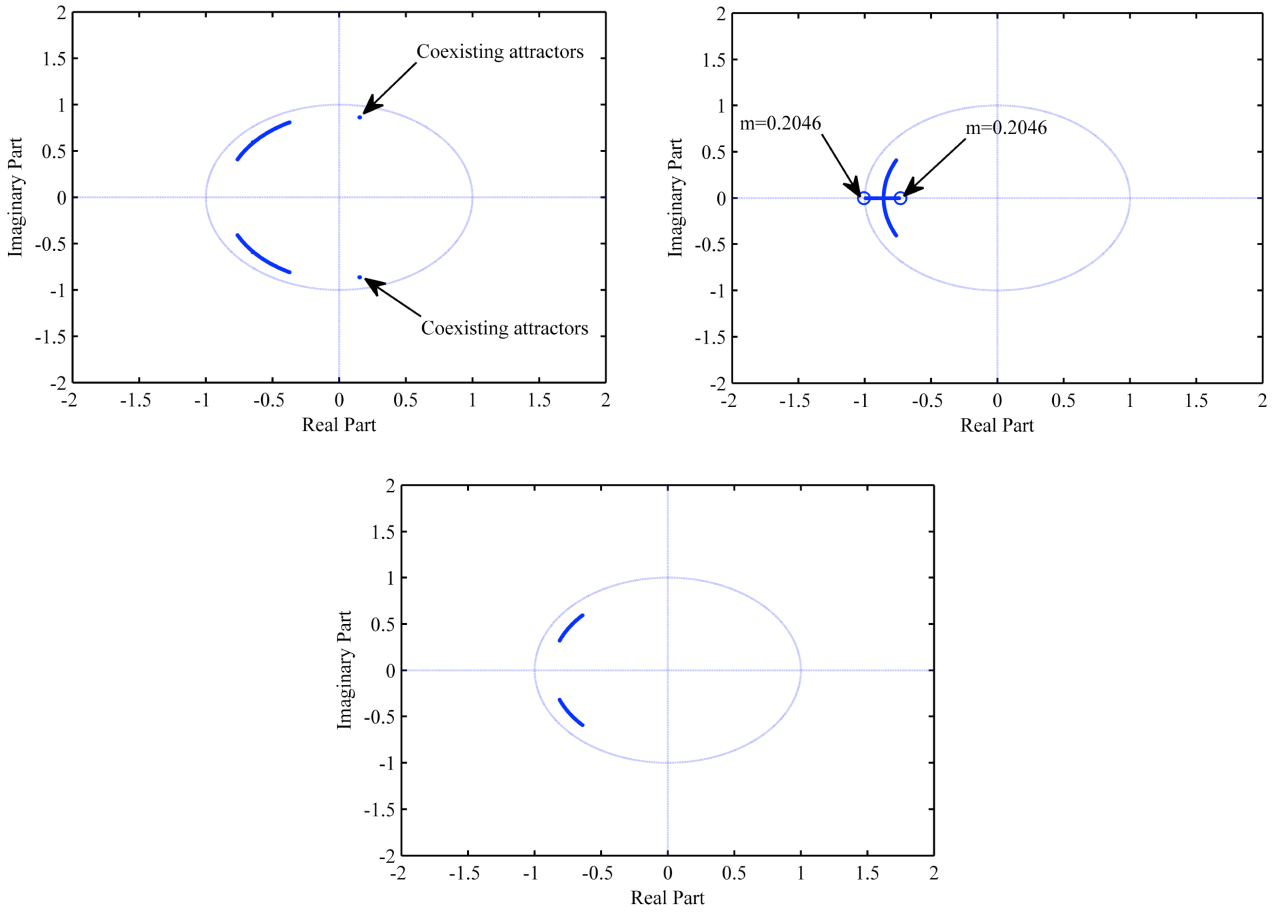

Figure 7. Locus of characteristic multipliers, corresponding to variations of the control intensity m and the input voltage V_{in}: (a) locus of characteristic multipliers for $m = 0.4 - 0.25$, $V_{in} = 35\,V$, $\gamma = 4$; (b) locus of characteristic multipliers for $m = 0.25 - 0.2046$, $V_{in} = 35\,V$, $\gamma = 4$; (c) locus of characteristic multipliers for $V_{in} = 35 - 40\,V$, $m = 0.3$, $\gamma = 4$.

through –1, indicating a period-doubling bifurcation. The critical bifurcation point is $m = 0.2046$, which means that the stable period-1 orbit is to lose stability.

According to the above analyses, chaos in the Buck converter is controlled to the stable period-1 orbit when $0.2046 < m < 1$, $\gamma = 4$.

The locus of characteristic multipliers for V_{in} = 35–40 V is shown in Figure 7c. It is shown that when V_{in} = 35–40 V, $m = 0.3$, and $\gamma = 4$, the Buck converter after being controlled is in the stable period-1 orbit. That is, the stability zone of the Buck converter can be widened by applying the self-feedback chaos control method.

Output voltage waveforms during a switching period $T = 400\,\mu s$ are described by Figure 8, corresponding to $m = 0.3$, 0.15, 0.072 and $\gamma = 0.4$. With the control intensity $m = 0.072 < 0.15 < 0.3$ increasing, slopes of curves decrease. Figure 8 confirms that the larger m is, the smoother the system response is, as mentioned in Section 4. Here, the system response is the output voltage.

Figure 9 shows that while taking $\gamma = 0.4$, 40, 400 and $m = 0.3$ the slopes of output voltage waveforms are almost consistent. This means that γ has almost no influence on oscillation of the output voltage even though this parameter has a significant variation. However, a slight variation of the control intensity m has a remarkable effect on stationarity of the output voltage.

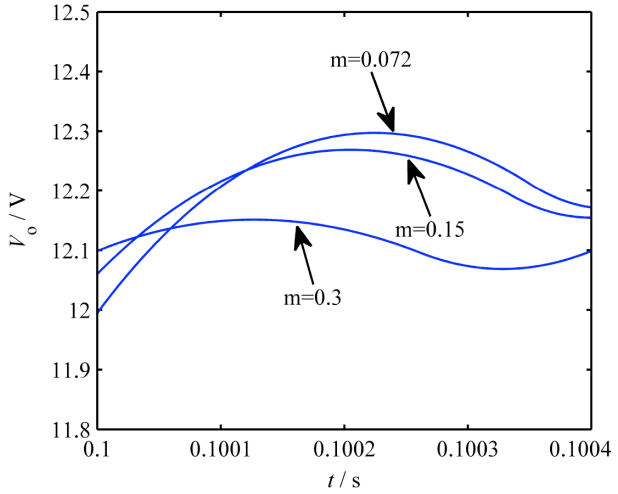

Figure 8. Output voltage waveforms during a switching period $T = 400\,\mu s$ when $m = 0.3$, 0.15, 0.072 and $\gamma = 0.4$.

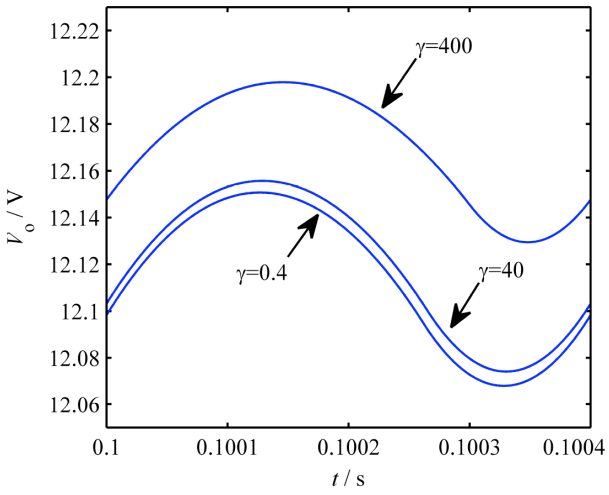

Figure 9. Output voltage waveforms during a switching period $T = 400\,\mu s$ when $\gamma = 0.4$, 40, 400 and $m = 0.3$.

In the process of tuning parameters, $0 < \gamma < \frac{V_{in}}{L}$ is taken as a minor (secondary) parameter and is roughly adjusted. $0 < m < 1$ is regarded as the main (principal) parameter and is accurately tuned. Besides, regulation of m does not rely on circuit parameters of the Buck converter, which makes adjustment of m flexible.

Certainly, the inductor current can also be considered as the system response and the same results can be obtained. This case will not be given in detail.

In the following text, without loss of generality, taking $\gamma = 4$ and $m = 0.3$, the stable period-1 orbit is discussed.

Figure 10 shows the transition from the chaotic motion to the stable period-1 motion. Without applying the self-feedback chaos control method ($t < 0.02\,s$), the Buck converter is working in the chaotic regime. Applying this method and after a transient, the stable regime is reached.

For clearly viewing the stable period-1 orbit, blowing up the interval $t = [0.1, 0.1035]\ s$ in Figure 10, we obtain the output voltage waveform of the stable period-1 orbit (see Figure 11). In this interval, the system is under the stable regime.

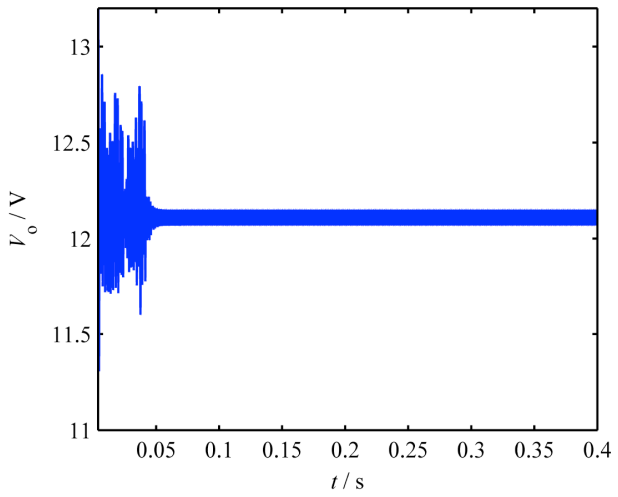

Figure 10. Transition from the chaotic motion to the stable period-1 motion, the output voltage versus time, with $\gamma = 4$, $m = 0.3$.

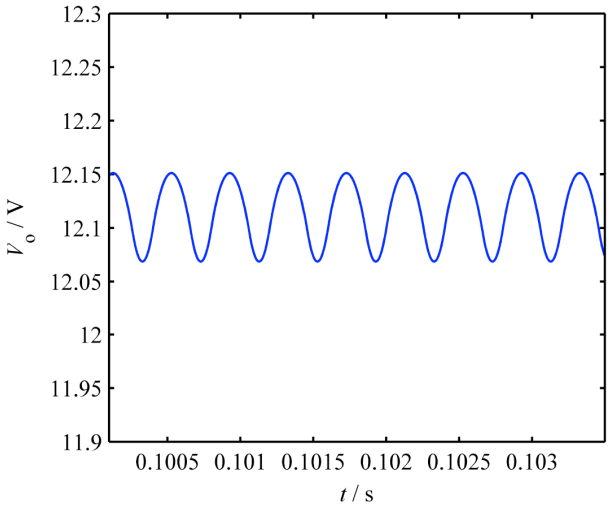

Figure 11. Output voltage waveform of the stable period-1 orbit with $\gamma = 4$, $m = 0.3$, $t = [0.1, 0.1035]\ s$.

When the Buck converter is in the stable period-1 orbit, the periods of the output voltage, the inductor current (see Figure 12), and the switching logic u (see Figure 13) are equal to the switching period $T = 400\mu s$. That is, the system steady-state waveforms are periodic with the same period as the sawtooth voltage V_{ramp}.

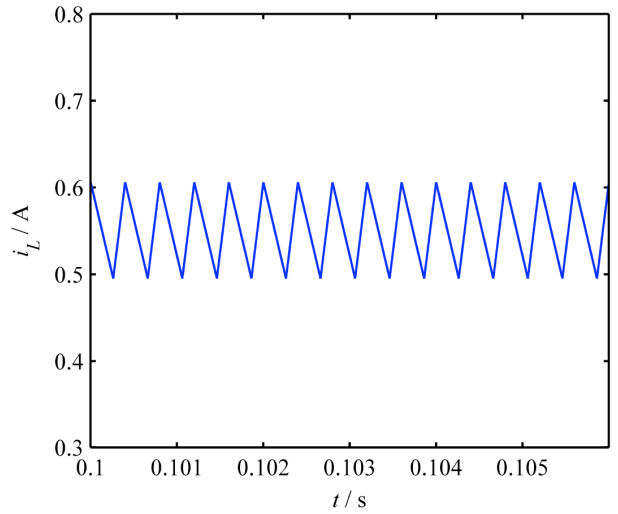

Figure 12. Inductor current waveform of the stable period-1 orbit with $\gamma = 4$, $m = 0.3$.

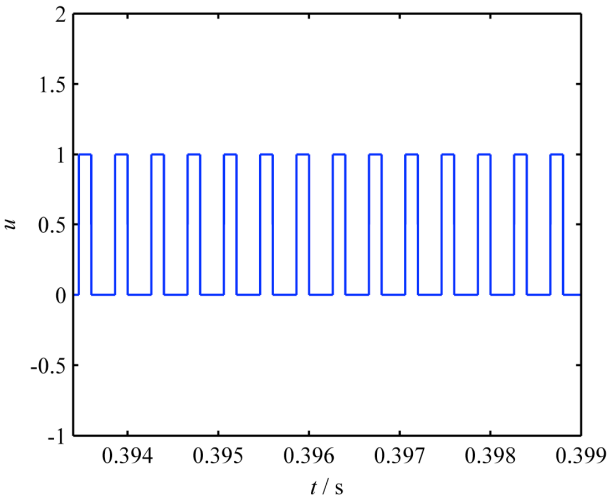

Figure 13. Switching logic diagram of the stable period-1 orbit with $\gamma = 4$, $m = 0.3$.

The phase plot of the stable period-1 orbit is a closed curve (see Figure 14). If we want to see how the output voltage and the inductor current are varying with t, we need a tridimensional representation (t, V_o, i_L). When increasing $t \geq 0.1$, the curve described in the space gives the stable solution of the Buck converter (see Figure 15). It can be observed that (t, V_o, i_L) is also regular.

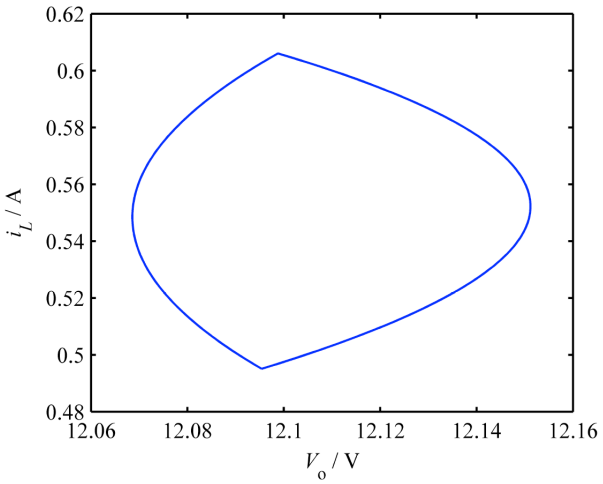

Figure 14. Phase portrait of the stable period-1 orbit with $\gamma = 4$, $m = 0.3$.

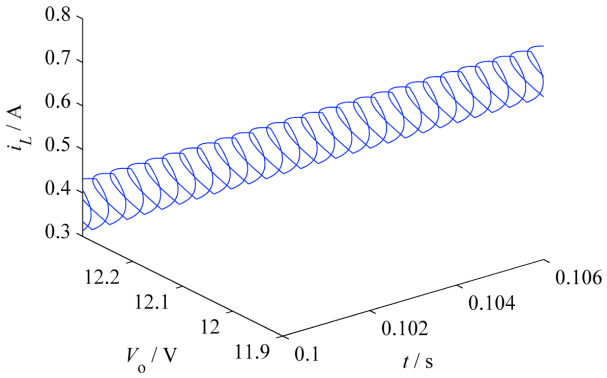

Figure 15. Tridimensional representation (t, V_o, i_L) of the stable period-1 orbit with $\gamma = 4$, $m = 0.3$.

As shown in Figure 16, the control voltage V_{con} is compared with the sawtooth voltage V_{ramp}. In each cycle of V_{con}, there is one sawtooth voltage V_{ramp} waveform. That is, the period of V_{con} is T. From Eq. (4) in Section 2, if $V_{ramp} > V_{con}$, then the controlled switch G is on; if $V_{ramp} < V_{con}$, then the controlled switch G is off. With the help of Eq. (4) and according to Figure 16, it is readily concluded that the controlled switch G is on (off) for one time in a cycle of V_{con} while the Buck converter runs in the stable period-1 orbit.

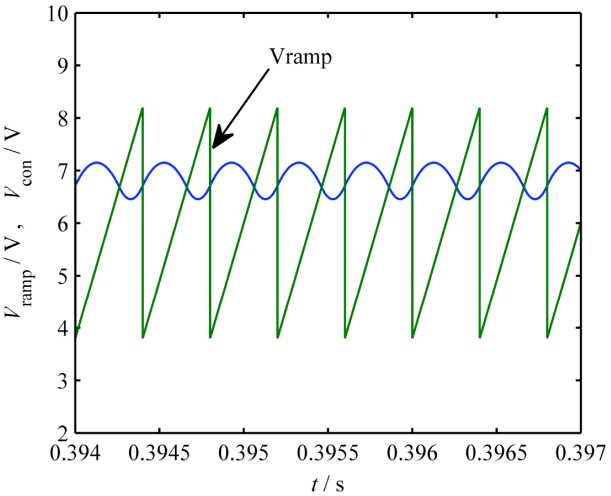

Figure 16. Comparison graph of the stable period-1 orbit with $\gamma = 4$, $m = 0.3$.

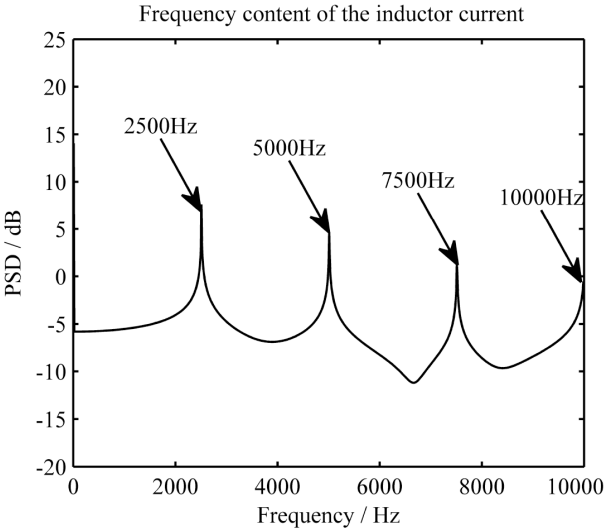

Figure 17. Power-spectral density (PSD) of the stable period-1 orbit with $\gamma = 4$, $m = 0.3$.

When the Buck converter after being controlled is under the stable period-1 orbit, the PSD based on FFT exhibits some spikes at $\frac{j}{T} = 2500j$ where $j = 1, 2, 3, 4$ (see Figure 17). This means that inductor current ripples are degraded compared with the PSD of the chaotic state. The Poincare section of the stable period-1 orbit has only one point (see Figure 18).

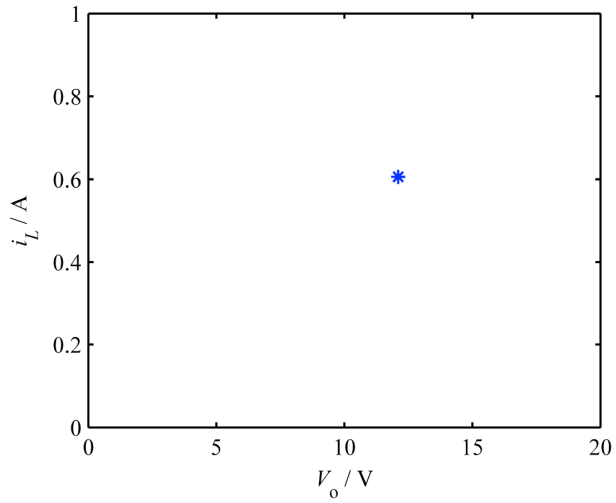

Figure 18. Poincare section of the stable period-1 orbit with $\gamma = 4$, m= 0.3.

7. Conclusions

It is proven that the self-feedback chaos control method can stabilize the chaotic behavior in the Buck converter to the stable period-1 orbit by adjusting the controller's parameters. Moreover, the stability region of the Buck converter is widened and the voltage conversion efficiency is improved using this chaos control method. Note that a large variation of γ has little influence on the system response. However, a slight variation of the control intensity m has a remarkable effect on the system response. Hence, in the process of tuning the controller's parameters, initially the minor parameter γ is treated as a fixed value and then the control intensity m as the main parameter is finely selected in the interval $(0.2046, 1)$.

The self-feedback chaos control method is independent of state variables of the Buck converter. Hence, this method is useful when state variables of the system cannot be readily measured.

In future work, this method can also be used to remove the chaotic phenomena existing in other hybrid dynamical systems such as the flyback converter, the Ćuk converter, and the power factor correction circuit.

Acknowledgment

This work was supported by the Inner Mongolia University of Technology Foundation (ZD201520) and the Natural Science Foundation of Inner Mongolia Autonomous Region of China (2017BS0603).

References

[1] Chakrabarty, K.; Poddar, G.; Banerjee, S. *IEEE T. Power Electr.* **1996**, *11*, 439-447.

[2] Li, Z. H.; Zhou, G. H.; Liu, X. T.; Leng, M. R. *Acta Phys. Sin.* **2015**, *64*, 1805011-18050110.

[3] Chang, C. Y.; Zhao, X.; Yang, F.; Wu, C. E. *Chin. Phys.* B **2016**, *25*, 0705041-0705048.

[4] Ott, E.; Grebogi, C.; Yorke, J. A. *Phys. Rev. Lett.* **1990**, *64*, 1196-1199.

[5] Dattani, J.; Blake, J. C. H.; Hilker, F. M. *Phys. Lett. A* **2011**, *375*, 3986-3992.

[6] Franco, D.; Liz, E. *Int. J. Bifurcat. Chaos* **2013**, *23*, 13500031.

[7] Braverman, E.; Chan, B. *Chaos* **2014**, *24*, 0131191.

[8] Braverman, E.; Franco, D. *Phys. Lett. A* **2015**, *379*, 1102-1109.

[9] Zhou, Y. F.; Tse, C. K.; Qiu, S. S.; Lau, F. C. M. *Int. J. Bifurcat. Chaos* **2003**, *13*, 3459-3471.

[10] Kavitha, A.; Uma, G. *Int. J. Control Autom. Syst.* **2010**, *8*, 1320-1329.

[11] Batlle, C.; Fossas, E.; Olivar, G. *Int. J. Circuit Theor. App.* **1999**, *27*, 617-631.

[12] Abbasi, H. R.; Gholami, A.; Rostami, M.; Abbasi, A. *Iran. J. Elec. Electron. Eng.* **2011**, *7*, 42-51.

[13] Lu, W. G.; Zhou, L. W.; Luo, Q. M. *Chin. Phys.* **2007**, *16*, 3256-3261.

[14] Lu, W. G.; Zhou, L. W.; Luo, Q. M.; Zhang, X. F. *Phys. Lett. A* **2008**, *372*, 3217-3222.

[15] Lu, W. G.; Zhou, L. W.; Wu, J. K. *Chin. Phys. Lett.* **2009**, *26*, 0305031-0305034.

[16] Lu, W. G.; Zhou, L. W.; Luo, Q. M.; Wu, J. K. *Int. J. Circuit Theor. App.* **2011**, *39*, 159-174.

[17] Chakrabarty, K.; Banerjee, S. *Phys. Lett. A* **1995**, *200*, 115-120.

[18] Fang, C. C.; Abed, E. H. *Nonlinear Dyn.* **2002**, *27*, 295-309.

[19] Jia, M. M.; Zhang, G. S.; Niu, H. *Acta Phys. Sin.* **2013**, *62*, 1305031-1305038.

[20] Dai, D.; Tse, C. K.; Ma, X. K. *IEEE T. Circuits-I* **2005**, *52*, 1632-1643.

[21] Luo, X. S.; Wang, B. H.; Zou, Y. L. *Adv. Mech.* **2003**, *33*, 471-482.